J. Membrane Biol. 90, 13–20 (1986)

The Journal of
Membrane Biology

Mechanism of Anion-Cation Selectivity of Amphotericin B Channels

Marina P. Borisova, Rafik A. Brutyan, and Lev N. Ermishkin
Institute of Biological Physics, USSR Academy of Sciences, Pushchino, Moscow Region, USSR

Summary. Zero current potential and conductance of ionic channels formed by polyene antibiotic amphotericin B in a lipid bilayer were studied in various electrolyte solutions. Nonpermeant magnesium and sulphate ions were used to independently vary the concentration of monovalent anions and cations as well as to maintain the high ionic strength of the two solutions separated by the membrane. Under certain conditions the channels select very strongly for anions over cations. They are permeable to small inorganic anions. However, in the absence of these anions the channels are practically impermeable to any cation. In the presence of a permeant anion the contribution of monovalent cations to channel conductance grows with an increase in the anion concentration. The ratio of cation-to-anion permeability coefficients is independent of the membrane potential and cation concentration, but it does depend linearly on the sum of concentrations of a permeant anion in the two solutions. These results are accounted for on the assumption that a cation can enter only an anion-occupied channel to form an ionic pair at the center of the channel. The cation is also assumed to slip past the anion and then to leave the channel for the opposite solution. This model with only few parameters can quantitatively describe the concentration dependences of conductance and zero current potential under various conditions.

Key Words lipid bilayer · polyene antibiotics · single channels · ion selectivity · ion interaction

Introduction

At present it is generally accepted that ion transport in *cation-selective channels* of muscular and axonal membranes, as well as in gramicidin channels in a lipid bilayer, cannot be accounted for by classic electrodiffusion, and it should be considered as ion migration through a series of binding sites. This new approach takes into account the ionic interaction in the channel due to competition for binding sites and electrostatic repulsion between cations (Hille, 1979; Eisenman & Horn, 1983). Much less is known about ion transfer in channels permeable to both cations and anions such as symmetrical channels created in a lipid bilayer by the polyene antibiotics amphotericin B and nystatin. Anion-to-cation selectivity of these channels as measured by dilution potentials is usually not very high, so that one might think that the ability of these channels to transport ions of any sign is due to the relatively large diameter of the pores (about 8 Å) (Andreoli, Dennis & Weigl, 1969; Finkelstein & Holz, 1973) and the transport of ions of each type does not depend on the counterion.

Here we show that this is not the case. Under certain conditions the amphotericin B channels exhibit a very high selectivity to anions over cations and the value of cation-anion selectivity is dependent on the concentration of a permeant anion but not of a cation. Replacing the permeant ions by nonpermeant Mg^{2+} and sulphate, we could independently vary the concentration of monovalent anions and cations and simultaneously maintain the high ionic strength of the solutions in order to minimize the effect of ion redistribution in the field of the membrane surface charges on the zero current potential and channel permeability being measured.

Materials and Methods

Membranes were formed of total brain phospholipids with cholesterol in *n*-heptane (20 : 1 mg per 1 ml). The procedure of lipid isolation and the monitoring of single channels were as described previously (Ermishkin, Kasumov & Potseluyev, 1977). Amphotericin B (dissolved in dimethylsulfoxide) was added in equal concentrations to both aqueous solutions, and its concentration was carefully adjusted within 2–3 nM for single channel monitoring and about 20 nM for measuring the zero current potential and integral conductance. At 20 nM concentration the integral conductance value (measured at 10 mV) did not exceed 10 nS for any solution composition (hole diameter 0.2 mm). As the low conductance of single channels cannot be measured in the linear region of the current-voltage curve at low concentration of permeant ions, it was obtained in the following indirect way: The membrane was formed in the solutions of high ionic strength with amphotericin B added. After conductance reached an almost steady-state level (conductance increase did not exceed 10% for

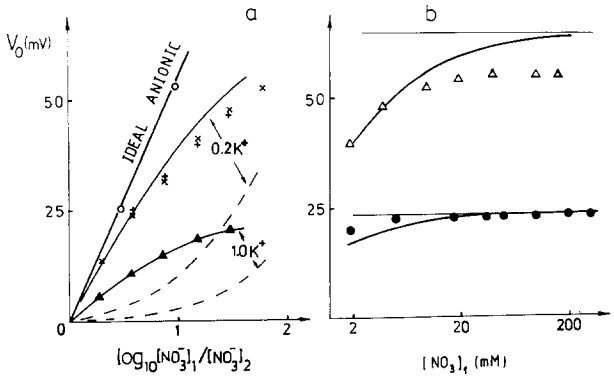

Fig. 1. (*a*) Dependence of zero current potential on the logarithm of the ratio of nitrate concentrations in the two solutions at two K-ion concentrations. Initially both solutions contained: (○) 0.5 M $MgSO_4$ + 2 mM $Mg(NO_3)_2$; (▲) 0.5 M K_2SO_4 + 2 mM $Mg(NO_3)_2$; (×) 0.1 M K_2SO_4 + 0.4 M $MgSO_4$ + 2 mM $Mg(NO_3)_2$. $Mg(NO_3)_2$ was added to solution 1. (+) Initially solution 1 contained: 0.1 M K_2SO_4 + 0.4 M $MgSO_4$ + 128 mM $Mg(NO_3)_2$; and solution 2: 0.1 M K_2SO_4 + 0.4 M $MgSO_4$ + 2 mM $Mg(NO_3)_2$; $Mg(NO_3)_2$ was added to solution 2 up to 32 mM concentration. V_o = potential in solution 1 minus potential in solution 2. Solid curves are calculated by Eq. (11) with $\beta_c \gg \nu$ and $L_{KNO_3} = 0.8$ M^{-1}. (*b*) Dependence of zero current potential on nitrate concentration in one of the solutions (solution 1). No nitrate was added to the other solution. Both solutions contained: (Δ) 0.1 M K_2SO_4 + 0.4 M $MgSO_4$; (●) 0.5 M K_2SO_4. Thin lines are calculated by Eq. (11) with $A_2 = 0$ and $L_{KNO_3} = 0.8$ M^{-1}. Thick lines are calculated by Eq. (11) with $A_2 = 0.2$ mM. Dashed lines in *a* are calculated by Eq. (1) with concentration-independent $r_{KNO_3} = 0.37$

5 min), the "instantaneous" changes in conductance in response to addition of salts of the monovalent ions under study were measured with intensive stirring of both solutions. Following the final addition of the salt, the current-voltage characteristic of this membrane was recorded up to 200 mV. The single channel conductance was then determined in a separate experiment with the same salt concentration and membrane potential (200 mV). This conductance was used as a scale of the conductance at low potential values. So we assumed that the "instantaneous" changes in the membrane conductance caused by the changes in the salt composition of the solutions are entirely due to the changes in the conductance of channels but not their number. This assumption is based upon the following observations: (i) under constant ion strength of solutions the antibiotic concentration required for single channels to be observed does not depend on the type and concentration of permeant ions; (ii) formation and dissociation of the channels are slow processes (over 40 min) (Ermishkin et al., 1976, 1977), and even if the equilibrium in the channel formation reaction is shifted due to changes in the salt composition, the number of channels does not change significantly during the several minutes of our measurement time.

A pair of electrodes, each composed of Ag-AgCl-KCl-agar-agar-bridge filled with 0.5 M $MgSO_4$ or K_2SO_4, was used. In all experiments 0.5 M K_2SO_4 or 0.5 M $MgSO_4$ was present in both solutions. The pH of all aqueous solutions was adjusted to 6.0. No buffer was added. All measurements were carried out at room temperature (22–23°C).

Results

Zero Current Potential

The dilution potential measurements on the membrane with two-sided amphotericin B channels indicate preferential but not ideal anionic selectivity (Cass, Finkelstein & Krespi, 1970; Ermishkin et al., 1976, 1977). When the membrane was interposed between 3 and 1 M KCl solutions, $V_o = -19.6$ mV, and in the case of 2 and 2/3 M KNO_3, $V_o = -11.5$ mV, both values being lower than the anticipated value $E_a = -28$ mV for an ideal anionic electrode. It is rather convenient to describe the relative contributions of cations and anions to the conductance by the ratio (r_{ca}) of the channel permeability coefficients for cations (P_c) and anions (P_a). In case of 1 : 1-valent electrolyte the ratio can be found from the Goldman-Hodgkin-Katz equation:

$$V_o = \frac{RT}{F} \ln \frac{r_{ca}C_1 + A_2}{r_{ca}C_2 + A_1}, \quad r_{ca} = P_c/P_a \qquad (1)$$

where C_1, C_2, A_1 and A_2 are concentrations of monovalent ions in the solutions 1 and 2, respectively.

Substituting the given V_o values into this equation one finds:

$$r_{KCl} = 0.15, \; r_{KNO_3} = 0.37.$$

In the extreme case of independent transport of ions, e.g. at such low concentrations that the simultaneous appearance of any two ions in the channel can be neglected, P_c and P_a, and consequently r_{ca}, should not be dependent on ion concentration. Hence, the dependence of r_{ca} on ion concentration can be used for evaluation of the degree and nature of the cation-anion interaction in the channel. The following experiment indicates r_{ca} dependence on the permeant anion concentration. If only 4 mM KCl was added to one of the solutions (both of them containing 0.5 M K_2SO_4), a zero current potential of 57 mV was observed (+ in solution with chloride). According to Eq. (1): $r_{KCl} = 4.4 \times 10^{-4}$, which is considerably lower than the value 0.15 estimated from the dilution potential at high concentrations of chloride.

The data of Fig. 1 with nitrate as a permeant ion also show that the behavior of the zero current potential is inconsistent with the concentration-independent permeability ratio. Figure 1*a* shows V_o *versus* nitrate concentration in one of the solutions. In the other solution the nitrate concentration was

kept constant and equal to 256 (+) or 4 mM in all other cases. In the absence of monovalent cations the nitrate concentration gradient resulted in V_o values which were close to those predicted by the Nernst equation for an ideal nitrate electrode in spite of the high (0.5 M) $MgSO_4$ concentration (open circles). Therefore the amphotericin B channels are much less permeable to magnesium and sulphate ions than to nitrate. In the presence of 0.5 M K_2SO_4 the nitrate gradient leads to lower V_o values due to K^+ contribution to the conductance, and the difference between the zero current potential and that of an ideal anion electrode increases with an increase in the potassium ion concentration.

The dashed lines in Fig. 1 correspond to the concentration-independent $r_{KNO_3} = 0.37$. These curves are below the corresponding experimental ones. It means that under the given experimental conditions the values of r_{KNO_3} are lower than 0.37. The experimental curves tend to saturation at high A_1 concentration, whereas the ones calculated by Eq. (1) with constant r_{KNO_3} values should asymptotically approach the straight lines with the slope of 58 mV for the 10-fold change of A_1. In another experiment (*see* Fig. 1*b*) nitrate was added to only one of the solutions. In spite of high K^+ concentration, the addition of 2 mM nitrate results in a potential of about 20 mV. Substitution of this value into Eq. (1) gives $r_{KNO_3} = 0.0018$. An increase in the nitrate concentration was shown to slightly affect the potential in contrast to what was expected at constant r_{ca}. This means that r_{ca} increases with nitrate concentration when K^+ concentration is constant.

Another interesting peculiarity of V_o dependence on the anion concentration is illustrated in Fig. 1*a* with 0.2 M K^+. The points obtained at different A_2 concentration, 4 mM (×) and 256 mM (+), fit the same curve, indicating that V_o value is not dependent on the absolute values of anion concentrations in the solutions but it does depend on their $A_1 : A_2$ ratio. So in next experiment the concentrations of nitrate in the two solutions were increased in such a way that their ratio was kept constant and equal to 3. In this case V_o value remained constant within a wide range of anion concentration (*see* Fig. 4*a*).

The values of r_{ca} for two concentrations of a permeant cation can be obtained on the basis of the data given in Fig. 1. The data show that a decrease in K concentration results in higher V_o values. However, r_{ca} values calculated by Eq. (1) do not practically depend on K concentration at any given anion concentration, e.g. at 2 mM nitrate $r_{KNO_3} = 0.0018$ and 0.0026 with 1 and 0.2 M K^+, respectively, and at 20 mM nitrate $r_{KNO_3} = 0.013$ for both K^+ concentrations. Figure 2 shows the results of another experiment on the effect of cation concentration (NH_4^+) on V_o and r_{ca} values. The membrane was formed in 0.5 M $MgSO_4$ + 10 mM $Mg(NO_3)_2$ solutions. Then the nitrate concentration in one of the solutions was increased threefold. A zero current potential close to the nitrate equilibrium one was obtained. Ammonium sulphate was then added in equal concentrations to both solutions, which resulted in a decrease of V_o observed (*see* Fig. 2*a*). The calculated value of $r_{NH_4NO_3}$ shown in Fig. 2*b* was approximately the same for a wide range of ammonium concentrations, showing only a slight decrease at high concentrations.

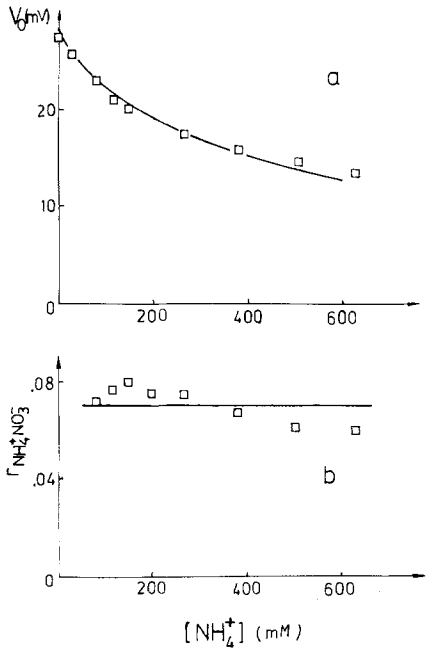

Fig. 2. (*a*) Zero current potential *versus* ammonium ion concentration in aqueous solutions. Initially one of the solutions contained 0.5 M $MgSO_4$ + 10 mM $Mg(NO_3)_2$ and the other 0.5 M $MgSO_4$ + 30 mM $Mg(NO_3)_2$. Ammonium sulphate was added in equal concentrations to both solutions. V_o = potential of solution with higher nitrate concentration minus the potential of the other solution. (*b*) Dependence of $r_{NH_4NO_3}$ on ammonium ion concentration calculated from the data of Fig. 2*a* by Eq. (1). Solid lines in *a* and *b* correspond to Eq. (1) with $r_{NH_4NO_3} = 0.07$

In Fig. 3 r_{ca} values from the data of Figs. 1, 2 and 4 are plotted as a function of the sum of concentrations of a permeant anion in the two solutions. Both for chloride and nitrate the points fall on the straight lines with a unit slope indicating that $r_{ca} \sim (A_1 + A_2)$.

As r_{KNO_3} were obtained for the different V_o values (up to 55 mV), Fig. 3 also shows only a slight (if

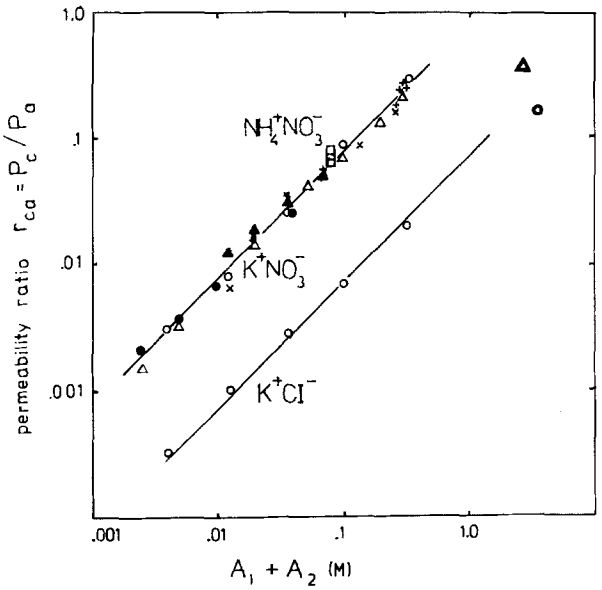

Fig. 3. Linear dependence of r_{ca} on the sum of concentrations of a monovalent anion in the two solutions r_{ca} values are calculated by Eq. (1) from the data of Figs. 1, 2 and 4*a* (same symbols). (●) r_{KCl} and (▲) r_{KNO_3} are from the data on dilution potentials (Ermishkin et al., 1977) (different ionic strength of the two solutions); (□) NH_4NO_3. Straight lines correspond to $r_{ca} = L_{ca}(A_1 + A_2)$ with $L_{KNO_3} = 0.80$; $L_{KCl} = 0.07$ M^{-1}

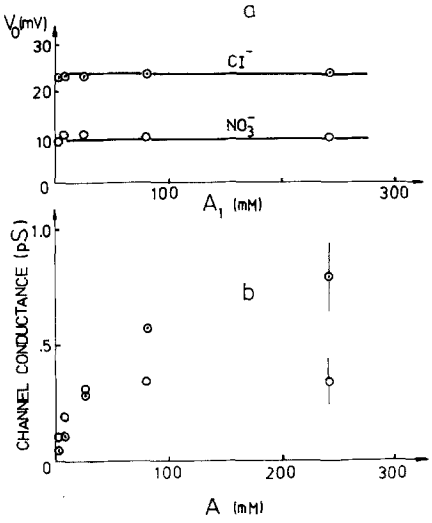

Fig. 4. (*a*) Zero current potential *versus* concentration of chloride or nitrate in one of the solutions. In the other solution the concentration of the same anion is three times as low. Both solutions contained 0.5 M K_2SO_4. Straight lines correspond to Eq. (12) with L_{ca} values from Eq. (14). V_o = potential in the solution with higher anion concentration minus the potential in the other solution. (*b*) Channel conductance depending on monovalent anion concentration in aqueous solutions at constant (0.5 M K_2SO_4) concentration of K ions. For every anion V_o and G values were obtained in the same experiment. First, V_o was measured with 1 and 3 mM chloride (or nitrate). Then KCl (KNO_3) was added to make anion concentration in both solutions equal to 3 mM and the conductance was measured, etc. Points with vertical bars in Fig. 4*b* correspond to mean and SD channel conductance at zero current. They are based on observation of 20 channels at 200 mV and (*I-V*) curve

any) dependence of the permeability ratio on the membrane potential.

Channel Conductance

The measurements of zero current potential make it possible to determine the ratio r_{ca} of permeability coefficients only. In order to evaluate separately the concentration dependence of cation and anion permeability, the conductance measurements should be carried out. The dependencies of the single amphotericin B channel conductance on electrolyte concentration were previously described (Ermishkin et al., 1977). For many 1 : 1-valent electrolytes these dependencies were monotonous with saturation at high salt concentrations. The measurements were carried out at high membrane potentials and a variable ionic strength of solutions. Figure 4*b* presents the data on conductance which are more suitable for theoretical treatment. They were obtained at high and almost constant ionic strength solutions and low (10 mV) membrane potential (*see* Materials and Methods).

The plots in Fig. 4*a* represent an increase in the channel conductance after the addition of monovalent anions in equal concentrations to 0.5 M K_2SO_4 solutions. Though the solutions contained high concentrations of K^+ the addition of even low chloride or nitrate concentrations resulted in a considerable increase in the conductance. For example, after the addition of 3 mM nitrate the channel conductance increased 7.4-fold and after the addition of 3 mM chloride, fivefold.

Using the Goldman-Hodgkin-Katz equation (1) and the data of Fig. 4*a* the total channel conductance can be subdivided into the cation and anion components. Note that using Eq. (1) is based on the assumption that the cation and anion fluxes can be described by the following equations

$$j_c = P_c(C_2e^{\varphi/2} - C_1e^{-\varphi/2})$$
$$j_a = P_a(A_2e^{-\varphi/2} - A_1e^{\varphi/2}),\ \varphi = VF/RT. \quad (2)$$

The equations require only that

$$j_c = 0$$

if

$$\varphi = \varphi_c = \ln C_1/C_2$$

and

$$j_a = 0$$

if

$$\varphi = \varphi_a = -\ln A_1/A_2.$$

In Eq. (2) the permeability coefficients (P_c and P_a) can be dependent on the membrane potential and permeant ion concentrations.[1] If $\Delta C \ll C_{1,2}$; $\varphi \ll 1$, then Eq. (2) becomes

$$j_c = P_c(C\varphi - \Delta C), j_a = -P_a(A\varphi + \Delta A) \quad (3)$$

where

$$\Delta C = C_1 - C_2, \Delta A = A_1 - A_2,$$
$$C = (C_1 + C_2)/2, A = (A_1 + A_2)/2.$$

Equating j_c and j_a we obtain the following equation for the zero current potential (reduced GHK equation)

$$\varphi_o = \frac{P_c C\varphi_c + P_a A\varphi_a}{P_c C + P_a A} = \frac{G_c\varphi_c + G_a\varphi_a}{G_c + G_a} \quad (4)$$

where

$$G_c = \frac{F^2}{RT} P_c C, G_a = \frac{F^2}{RT} P_a A \quad (5)$$

are the cation and anion components, respectively, of the total channel permeability:

$$G = G_c + G_a.$$

Under the experimental conditions of Fig. 4*a* ($\Delta C = 0$, $\varphi_c = 0$) Eq. (4) becomes

$$\varphi_o = \frac{G_a\varphi_a}{G_c + G_a}$$

or

$$\frac{\varphi_a - \varphi_o}{\varphi_o} = G_c/G_a. \quad (6)$$

[1] This condition Eq. (2) apparently limits the number of the permeability mechanisms under consideration. For example, let us consider a channel permeable only to ion complexes of a_2c^- (or ac_2^+), which are present in the aqueous solutions at low concentrations in equilibrium with c^+ and a^- ions. In this case the net fluxes of c^+ and a^- particles have no zero value at φ_c and φ_a, respectively, and they cannot be described by Eq. (2).

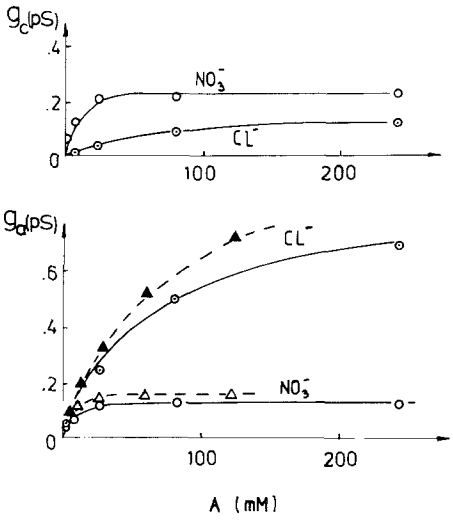

Fig. 5. Circles represent the cationic (top) and anionic components of channel conductance *versus* monovalent anion concentration at constant (0.5 M K_2SO_4) concentration of a permeant cation calculated by Eq. (7) from the data of Fig. 4. Triangles represent channel conductance depending on chloride (▲) or nitrate (△) concentration in the absence of a permeant cation (both solutions contain 0.5 M $MgSO_4$). Dashed lines are calculated for the two-barrier one-site model as

$$G = \frac{F^2}{2RT}\alpha_a A / \left(1 + \frac{\alpha_a}{\beta_a} A\right)$$

with

$\alpha_{Cl} = 0.68 \times 10^{-17}$; $\alpha_{NO_3} = 1.3 \times 10^{-17}$ l/sec;

$\beta_{Cl} = 5.4 \times 10^{-19}$; $\beta_{NO_3} = 1.0 \times 10^{-19}$ mole/sec. Solid lines are calculated by Eq. (16) with the same values of α_a and β_a and $L_{KCl} = 0.07$, $L_{KNO_3} = 0.8$ M^{-1}. Only one new parameter was adjusted to the experimental points: $\alpha_K/\beta_K = 0.12$ M^{-1}

As (I-V) curves are linear up to 30 mV, this equation is exact at φ_o, $\varphi_a \ll 1$ and accurate within 10% under the conditions of Fig. 4*a*.
Combining Eqs. (4) and (6) one gets

$$G_a = G\varphi_o/\varphi_a, G_c = G - G_a. \quad (7)$$

In Fig. 4*a* φ_a and φ_o are constant values, i.e., G_c/G_a is not dependent on the anion concentration whereas the total conductance ($G_c + G_a$) does increase with it. This means that the cation component of the channel conductance also depends on the anion concentration increasing in parallel with the anionic conductance. Figure 5 shows the separate anionic and cationic conductances calculated by Eq. (7) from the data of Fig. 4. The channel conductance dependences on chloride and nitrate in 0.5 M $MgSO_4$ in the absence of a permeant cation are also shown in Fig. 5*b*. Comparison of the curves shows that the presence of permeant K ions does

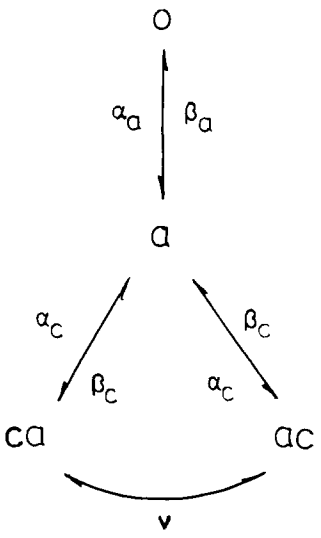

Fig. 6. Diagram of interconnections between channel states (for details *see* text)

not affect the curve shapes and causes only a slight decrease (if any) in the amplitude of the anionic component. By contrast the cationic component markedly increases with an increase in the permeant anion concentration. Below a simple model is considered which can describe the behavior of zero current potential and channel conductance, depending on the permeant ion concentrations.

Model

The data of Fig. 5 show that the monovalent anions can penetrate amphotericin B channels and the anionic conductance is almost independent of the presence of monovalent cations. On the contrary, in the absence of a permeant anion the channel is practically impermeable to K ions. The model should first of all describe the anion transfer through the channel. The dashed lines in Fig. are calculated for the symmetrical two-barrier one-site model of a channel. The model has only two parameters: rate constant of anion entry α_a and rate constant of anion release into solution β_a. The dashed curves properly represent the experimental data with the parameter values given in the legend to Fig. 5. Earlier it was shown (Borisova & Ermishkin, 1984) that such a simple model with a single ion site in the center of a channel could describe a number of experimental data: (i) independence of bianionic potentials of the anion concentration, (ii) applicability of the Ussing equation for the ratio of the unidirectional anion fluxes (Finkelstein & Holz, 1973), (iii) dependence of the shape of voltage-current characteristics on the permeant anion concentration. This enables us to use this model for the description of cation and anion transfer.

It is assumed that an anion (not a cation) can enter a vacant channel. Anion binding at the center of the channel seems to be mainly due to the electrostatic forces. According to the well known molecular model of the channel (Finkelstein & Holz, 1973; De Kruijff & Demel, 1974), its cavity is lined with hydrophilic chains of amphotericin B molecules with OH-dipoles oriented by positively charged protons to the center of the channel. These dipoles can induce a positive potential inside the pore, which favors anion binding and prevents a cation from entering the vacant channel. Anion binding compensates part of this potential and a cation can enter with the rate constant α_c. So, in the center of the channel the ion pair *ca* is formed if the cation enters from the left solution, and *ac* from the right. The formation of ion pairs in a channel is likely because the hydrophobic environment strongly enhances electrostatic interactions in it (Levitt, 1978). Thus it is assumed that the channel can be: (i) vacant (*o*), (ii) with a bound anion (*a*), (iii) with an ion pair (*ca*) or (iv) (*ac*). The diagram in Fig. 6 illustrates possible transitions among these states. We suggest that the anion and cation can exchange places in the ion pair with the rate constant ν. Monovalent inorganic ions have enough room to slip past each other in an amphotericin B channel of 8 Å diameter. Let us also assume that the only energetically favorable transition from the ion pair state occurs as a result of cation release with the rate constant β_c at zero membrane potential. The transitions *o*—*a*, *a*—*ac* and *a*—*ca* are potential-dependent. The transition *ca*—*ac* is assumed to be independent of the membrane potential.[2]

For the sake of simplicity all the barriers are considered to be symmetrical, meaning that the same fraction of the membrane potential (25%) drops from the channel entrance to the barrier height and from the barrier height to the binding site.[3]

Equations of anion (j_a) and cation (j_c) fluxes

[2] The difference in energy between the states *ca* and *ac* is $\Delta E = 2d/\ell \cdot V \cdot e$, where ℓ is the channel length, d the distance between the centers of the ions of a pair, e electron charge so that $\tilde{\nu}/\tilde{\nu} = \exp^{\Delta E/KT} = \exp(0{,}04 \cdot \varphi)$ with $l = 50$ Å; $d = 2$ Å. In the potential range considered ($V < 55$ mV) $\tilde{\nu} = \tilde{\nu}$ within 9%.

[3] In fact, the dependence of voltage-current curves on the anion concentration in magnesium chloride, iodide and nitrate is best described on the assumption that only 17% of the external field drops from the channel entrance to the top of the barrier for anions (Borisova & Ermishkin, 1984). However, the location of the top of the barrier for cations is not yet known.

through the left and right barriers appear as

$$j_a^{\text{left}} = \alpha_a A_1 N_o \exp\varphi/4 - \beta_a N_a \exp(-\varphi/4)$$
$$j_c^{\text{left}} = \alpha_c C_1 N_a \exp(-\varphi/4) - \beta_c N_{ca} \exp\varphi/4 \quad (8)$$
$$j_a^{\text{right}} = \beta_a N_a \exp\varphi/4 - \alpha_a A_2 N_o \exp(-\varphi/4)$$
$$j_c^{\text{right}} = \beta_c N_{ac} \exp(-\varphi/4) - \alpha_c C_2 N_a \exp\varphi/4 \quad (9)$$

where N_o, N_a, N_{ca}, N_{ac} are fractions of the channels in the corresponding state.

Steady-state distribution of the channels by the states can be found from the following conditions:

$$j_a^{\text{left}} = j_a^{\text{right}}; j_c^{\text{left}} = j_c^{\text{right}} = \nu(N_{ca} - N_{ac}) \quad (10)$$

and

$$N_o + N_a + N_{ca} + N_{ac} = 1.$$

Solving Eqs. (8) and (10) under the zero current condition $j_c = j_a$, we obtain an equation for the zero current potential

$$A_1 e^{\varphi_o/2} - A_2 e^{-\varphi_o/2} = \frac{\alpha_c}{\beta_a} \cdot \frac{A_1 e^{\varphi_o/4} + A_2 e^{-\varphi_o/4}}{\frac{\beta_c}{\nu} + e^{\varphi_o/4} + e^{-\varphi_o/4}} \cdot (C_1 e^{-\varphi_o/2} - C_2 e^{\varphi_o/2}). \quad (11)$$

Comparing Eqs. (11) and (2) at $j_c = j_a$ we can see that the expression on the right before the parentheses is r_{ca}, which in this model depends on the permeant anion concentration and membrane potential. At low potential values ($\varphi_o \ll 1$) Eq. (11) becomes

$$V_o = \frac{RT}{F} \ln \frac{L_{ca}(A_1 + A_2)C_1 + A_2}{L_{ca}(A_1 + A_2)C_2 + A_1} \quad (12)$$

which coincides with Eq. (1) if

$$r_{ca} = L_{ca}(A_1 + A_2), L_{ca} = \alpha_c/\beta_a \left(\frac{\beta_c}{\nu} + 2\right). \quad (13)$$

Here the selectivity coefficient L_{ca} does not depend on the permeant ion concentrations. The straight lines in Figs. 2 and 3 correspond to Eq. (13) if

$$L_{KCl} = 0.07, L_{KNO_3} = 0.80, L_{NH_4NO_3} = 0.88 \text{ M}^{-1}. \quad (14)$$

Let us consider the experimental results shown in Figs. 1, 2 and 4 on the basis of this model. Dividing both parts of Eq. (11) by A_2, we can see that the zero current potential depends on the A_1/A_2 ratio only, which agrees with the results in Figs. 1*a* (*compare* + and ×) and 4*a*. The straight lines in Figs. 2*a* and 4*a* are calculated using Eq. (12) at $A_1/A_2 = 3$, $C_1 = C_2$ with L_{ca} values from Eq. (14). The curves in Fig. 1 are calculated by Eq. (11) with the same L_{ca} values and at $\beta_c \gg \nu$. Considerable deviation of the calculated curves from the experimental points in Fig. 1*b* is apparently due to the presence of a monovalent anion admixture in $MgSO_4$ and K_2SO_4. As a result the assumed condition $A_2 = 0$ used for calculation was not met in the experiment. In a control experiment with 0.5 M $MgSO_4$ in both solutions the addition of 100 mM $Mg(NO_3)_2$ to one of them resulted in a zero current potential of 187 mV (+ in nitrate solution) which increased up to 215 mV after addition of 5 mM Ag_2SO_4 to the nitrate-free solution. We might expect such an effect if $MgSO_4$ solution contained 0.1–0.2 mM contaminant chloride which was subsequently bound by silver ions. The thick lines in Fig. 1*b* are calculated by Eq. (11) with $A_2 = 0.2$ mM. The correction for a monovalent anion admixture allows a better fit of the calculated curves to the experimental results.

Using r_{ca} dependence on the membrane potential, it is possible in principle to determine the rate-limiting step in the cation transfer. Here two alternatives may be considered: (i) cation release is a rate-limiting step ($\beta_c \ll \nu$) and the β_c/ν term in the denominator of Eq. (11) can be neglected; (ii) *ca—ac* limits cation transfer and the β_c/ν is the main term of the denominator. For the experiment shown in Fig. 1*b* we have calculated $V_o = 73$ mV in the first case and $V_o = 64$ mV in the second for the cation concentration of 0.2 M. The two values are close to each other and are slightly higher than the experimental one. So the possibility of a reliable determination of the rate-limiting step is ruled out. It should be noted that r_{ca} dependence on the membrane potential is strongly affected by the barrier height position and the discrepancy between the experimental and predicted values can be due to the assumption of barrier symmetry. Every curve in Fig. 1 is calculated with the arbitrary suggestion of $\beta_c \gg \nu$. At low potential values (with $C = 1$ M), Eq. (11) gives $V_o = 25$ mV regardless of the limiting stage in good agreement with the experimental data.

G_c and G_a are calculated as $G_c = Fj_c/RT$, $G_a = -Fj_a/RT$ from Eqs. (9) and (10) with $A_1 = A_2 = A$, $C_1 = C_2 = C$ and $\varphi \ll 1$:

$$G_c = \frac{F^2}{RT} \alpha_c \alpha_a ACN_o/\beta_a(2 + \beta_c/\nu) = \frac{F^2}{RT} L_{ca} \alpha_a ACN_o$$
$$G_a = \frac{F^2}{RT} \cdot \frac{\alpha_a}{2} AN_o$$
$$N_o^{-1} = 1 + \frac{\alpha_a}{\beta_a} A + 2 \frac{\alpha_c}{\beta_c} \cdot \frac{\alpha_a}{\beta_a} \cdot AC. \quad (15)$$

Both conductances are similarly dependent on the permeant anion concentration so that their ratio does not depend on A because in the present model both cationic and anionic conductance is proportional to the fraction N_a of anion-occupied channels. The curves in Fig. 5 calculated by Eq. (15) are in good agreement with the experimental results. So, the data on both zero current potential and single channel conductance can be adequately described by this model.

Conclusion

The above results show that permeation of cations through symmetric amphotericin B channels is strongly influenced by permeant anions. However, rather simple relations are observed between the ratio P_c/P_a and the concentrations of permeant ions; this ratio is almost independent of permeant cation concentration and linearly increases with an increase in the concentration of a permeant anion in the two solutions. Such asymmetric influence of cations and anions on the selectivity ratio indicates that the channels are intrinsically well permeable for anions and cations can pass only through the anion-occupied channels. The proposed mechanism of permeability and anion-cation selectivity can be realized in the channels that are wide enough to allow the ions of opposite signs to slip past each other. In a super-narrow channel with single-file ion movement the ionic pair formed by a cation and an anion moving in the opposite directions due to the membrane potential would block the channel.

High selectivity of amphotericin B channels to anions over cations at a low concentration of 1 : 1-valent electrolyte is determined by the dipole content of its cavity lined with OH-groups. At a high electrolyte concentration when most of the channels contain anions, the relatively high cationic permeability is due to a filter created by this anion. Note that cationic permeability of K and Na channels in nerves and muscles has long been believed to be due to the presence of a charged group in the channel. However, such a group in a narrow channel surrounded by a hydrophobic matrix could create a deep potential well for cations, limiting their transfer rate. Because of this and also as a result of the discovery of membrane-active antibiotics (gramicidin A, alamethicin, polyene antibiotics), which form channels without a localized charge, now it is assumed that the high selectivity in favor of ions of one sign is better created by means of a charge distributed along a set of dipoles. According to our results the cationic selectivity can be due to localized charge in at least not very narrow channels. And the high selectivity for cations over anions can be created not only by a negative charge covalently bound to the channel structure but also by the mobile charge of a permeant anion if this anion is tightly bound to the channel and makes it possible for many cations to slip past it.

References

Andreoli, N.E., Dennis, V.W., Weigl, A.M. 1969. The effect of amphotericin B on the water and nonelectrolyte permeability of thin lipid membranes. *J. Gen. Physiol.* **53**:133–155

Borisova, M.P., Ermishkin, L.N. 1984. The kinetic parameters for anion transport through amphotericin B channels. *Biol. Membranes (Russian)* **1**:537–540

Cass, A., Finkelstein, A., Krespi, V. 1970. The ion permeability induced in thin lipid membranes by the polyene antibiotics nystatin and amphotericin B. *J. Gen. Physiol.* **56**:100–124

De Kruijff, B., Demel, R.A. 1974. Polyene antibiotics-sterol interactions in membranes of *Acholeplasma laidlawii* cells and lecithin liposomes. *Biochim. Biophys. Acta* **339**:57–70

Eisenman, G., Horn, R. 1983. Ionic selectivity revisited: The role of kinetic and equilibrium processes in ion permeation through channels. *J. Membrane Biol.* **76**:197–225

Ermishkin, L.N., Kasumov, K.M., Potseluyev, V.M. 1976. Single channels induced in lipid bilayers by polyene antibiotics amphotericin B and nystatin. *Nature (London)* **262**:698–699

Ermishkin, L.N., Kasumov, K.M., Potseluyev, V.M. 1977. Properties of amphotericin B channels in a lipid bilayer. *Biochim. Biophys. Acta* **470**:357–367

Finkelstein, A., Holz, R. 1973. Aqueous pores created in thin lipid membranes by the polyene antibiotics nistatin and amphotericin B: *In:* Membranes. Lipid Bilayers and Antibiotics. Vol. 2, pp. 377–408. G. Eisenman, editor, Marcel Dekker, New York.

Hille, B. 1979. Rate theory models for ion flow in ionic channels of nerve and muscle. *In:* Membrane Transport Processes. Vol. 3, pp. 5–16. C.F. Stevens and R.W. Tsien, editors. Raven, New York

Levitt, D., 1978. Electrostatic calculations for an ion channel. *Biophys. J.* **22**:209–219

Received 1 April 1985; revised 22 August 1985